ORGANOMETALLICS

Mechanism of isomerization of rhenium alkylidene complexes [(.eta.5-C5H5)Re(NO)(PPh3)(:CRCHR'R")]+X- to alkene complexes [(.eta.5-C5H5)Re(NO)(PPh3)(RHC:CR'R")]+X-: an organometallic Wagner-Meerwein-type rearrangement

Christophe. Roger, Gerardo S. Bodner, William G. Hatton, and J. A. Gladysz

Organometallics, **1991**, 10 (9), 3266-3274• DOI: 10.1021/om00055a051 • Publication Date (Web): 01 May 2002

Organometallics is published by the American Chemical Society. 1155 Sixteenth Street N.W., Washington, DC 20036

a solid precipitate of 2 from pentane with an acceptable elemental analysis have failed. A common contaminant is 2,5-dimethyl-1,5-hexadiene, an impurity originating from the synthesis of C_4H_7MgCl. If this nonvolatile hydrocarbon is present in high concentrations, a dark blue oil will be obtained. ^1H NMR: Refer to Table II.

Acknowledgment. This work was supported by grants from the Robert A. Welch Foundation (Y-1076) and the donors of the Petroleum Research Fund, administered by the American Chemical Society. The efforts of a Research Assistant, Mrs. Su-Inn Ho, are also gratefully acknowledged.

Supplementary Material Available: A structure determination listing, tables of positional and isotropic thermal parameters (Table 1), bond lengths (Table 2), bond angles (Table 3), anisotropic temperature factors (Table 4), and H coordinates and isotropic displacement parameters (Table 5), and a peak by peak analysis of the COSY plots for 1 and 2 (20 pages); a listing of observed and calculated structure factors (Table 6) (4 pages). Ordering information is given on any current masthead page.

Mechanism of Isomerization of Alkylidene Complexes $[(\eta^5\text{-}C_5H_5)Re(NO)(PPh_3)(=CRCHR'R'')]^+X^-$ to Alkene Complexes $[(\eta^5\text{-}C_5H_5)Re(NO)(PPh_3)(RHC=CR'R'')]^+X^-$: An Organometallic Wagner–Meerwein-Type Rearrangement

Christophe Roger, Gerardo S. Bodner, William G. Hatton, and J. A. Gladysz*

Department of Chemistry, University of Utah, Salt Lake City, Utah 84112

Received March 20, 1991

Propylidene complex $[(\eta^5\text{-}C_5H_5)Re(NO)(PPh_3)(=CHCH_2CH_3)]^+PF_6^-$ ($\mathbf{1c}^+PF_6^-$) cleanly rearranges to propene complex $[(\eta^5\text{-}C_5H_5)Re(NO)(PPh_3)(H_2C=CHCH_3)]^+PF_6^-$ (C_6D_5Cl, 65–86 °C; $\Delta H^\ddagger = 27 \pm 1$ kcal/mol; $\Delta S^\ddagger = 3 \pm 3$ eu). Experiments with deuterated $\mathbf{1c}^+PF_6^-$ show a modest primary kinetic deuterium isotope effect ($k(=CHCH_2CH_3)/k(=CHCD_2CH_3) = 1.95–1.40$) but a considerable inverse secondary kinetic deuterium isotope effect ($k(Re=CH)/k(Re=CD) = 0.50–0.58$). A crossover experiment shows intramolecular hydride migration and the absence of PPh_3 ligand dissociation. Optically active $\mathbf{1c}^+PF_6^-$ rearranges with retention of configuration at rhenium, but the hydride shift is not stereospecific at the migration terminus. However, the rearrangement of isobutylidene complex $[(\eta^5\text{-}C_5H_5)Re(NO)(PPh_3)(=CHCH(CH_3)_2)]^+SO_3F^-$ to isobutylene complex $[(\eta^5\text{-}C_5H_5)Re(NO)(PPh_3)(H_2C=C(CH_3)_2)]^+SO_3F^-$ is highly stereoselective at the migration origin and terminus, and much faster than that of $\mathbf{1c}^+PF_6^-$ (CD_2Cl_2, 3–25 °C; $\Delta H^\ddagger = 21 \pm 1$ kcal/mol; $\Delta S^\ddagger = -3 \pm 3$ eu). Rearrangements of analogous pentylidene and cyclopentylidene complexes are also studied. An orbital symmetry analysis of these reactions is given.

Carbon–hydrogen bond activation is a focal point of research in organometallic chemistry. Several classes of hydrocarbon ligands have been found to participate in prototropic rearrangements near room temperature. For example, alkylidene complexes often undergo a 1,2-hydride migration to give alkene complexes (eq i).[1-10] Also, terminal alkyne complexes have been observed to rearrange to vinylidene complexes (eq ii).[11-13] Interestingly, eq i ($M=C \rightarrow \pi$) has a thermodynamic sense opposite to that of eq ii ($\pi \rightarrow M=C$).

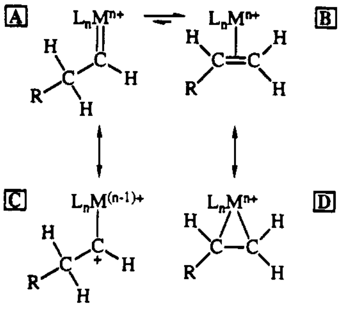

(i)

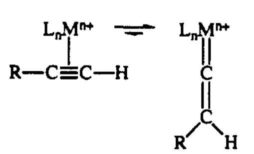

(ii)

---

(1) Brookhart, M.; Tucker, J. R.; Husk, G. R. *J. Am. Chem. Soc.* **1981**, *103*, 979; **1983**, *105*, 258.

(2) Marsella, J. A.; Folting, K.; Huffman, J. C.; Caulton, K. G. *J. Am. Chem. Soc.* **1981**, *103*, 5596.

(3) Bodnar, T.; Cutler, A. R. *J. Organomet. Chem.* **1981**, *213*, C31.

(4) Casey, C. P.; Miles, W. H.; Tukada, H. *J. Am. Chem. Soc.* **1985**, *107*, 2924.

(5) (a) Kremer, K. A. M.; Kuo, G.-H.; O'Connor, E. J.; Helquist, P.; Kerber, R. C. *J. Am. Chem. Soc.* **1982**, *104*, 6119. (b) Kuo, G.-H.; Helquist, P.; Kerber, R. C. *Organometallics* **1984**, *3*, 806.

(6) Hatton, W. G.; Gladysz, J. A. *J. Am. Chem. Soc.* **1983**, *105*, 6157.

(7) Freudenberger, J. H.; Schrock, R. R. *Organometallics* **1985**, *4*, 1937.

(8) Examples where the alkylidene complex is not directly observed: (a) Cutler, A.; Fish, R. W.; Giering, W. P.; Rosenblum, M. *J. Am. Chem. Soc.* **1972**, *94*, 4354. (b) Labinger, J. A.; Schwartz, J. *Ibid.* **1975**, *97*, 1596. (c) Casey, C. P.; Albin, L. D.; Burkhardt, T. J. *Ibid.* **1977**, *99*, 2533. (d) Fischer, E. O.; Held, W. *J. Organomet. Chem.* **1976**, *112*, C59. (e) Guerchais, V. *J. Chem. Soc., Chem. Commun.* **1990**, 534.

(9) Some conceptually related hydride migrations: (a) Casey, C. P.; Marder, S. R.; Adams, B. R. *J. Am. Chem. Soc.* **1985**, *107*, 7700. (b) Green, M.; Orpen, A. G.; Schaverein, C. J. *J. Chem. Soc., Chem. Commun.* **1984**, 37.

(10) Some analogous carbon migrations: (a) Bly, R. S.; Bly, R. K. *J. Chem. Soc., Chem. Commun.* **1986**, 1046. (b) Bly, R. S.; Bly, R. K.; Hossain, M. M.; Lebioda, L.; Raja, M. *J. Am. Chem. Soc.* **1988**, *110*, 7723. (c) Bly, R. S.; Silverman, G. S.; Bly, R. K. *Ibid.* **1988**, *110*, 7730. (d) Bly, R. S.; Wu, R.; Bly, R. K. *Organometallics* **1990**, *9*, 936. (e) Bly, R. S.; Raja, M. *Ibid.* **1990**, *9*, 1500.

(11) (a) Bruce, M. I. *Chem. Rev.* **1991**, *91*, 197. (b) Silvestre, J.; Hoffmann, R. *Helv. Chim. Acta* **1985**, *68*, 1461. (c) Pombeiro, A. J. L.; Richards, R. L. *Coord. Chem. Rev.* **1990**, *104*, 13.

(12) (a) Bullock, R. M. *J. Chem. Soc., Chem. Commun.* **1989**, 165. (b) Werner, H. *Angew. Chem., Int. Ed. Engl.* **1990**, *29*, 1077. (c) Werner, H.; Hampp, A.; Peters, K.; Peters, E. M.; Walz, L.; von Schnering, H. G. *Z. Naturforsch.* **1990**, *45b*, 1548.

(13) Kowalczyk, J. J.; Arif, A. M.; Gladysz, J. A. *Organometallics* **1991**, *10*, 1079.

0276-7333/91/2310-3266$02.50/0 © 1991 American Chemical Society

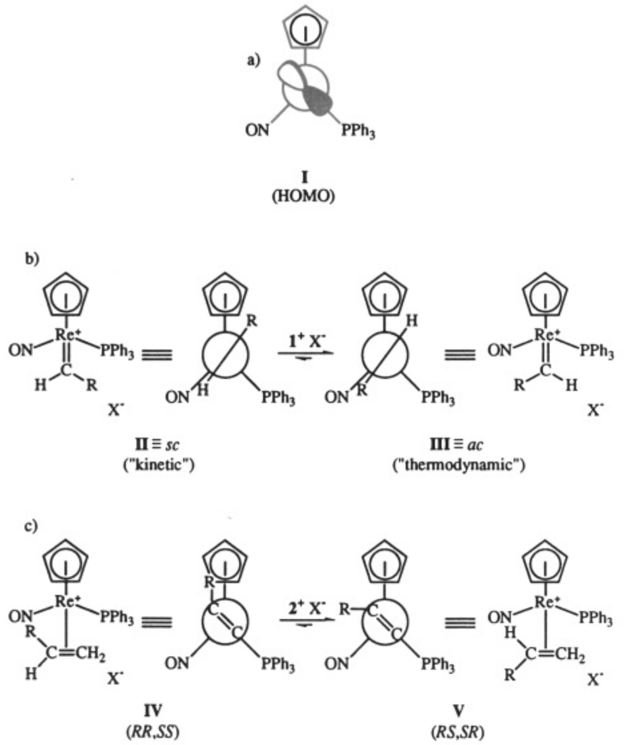

Figure 1. Comparison of the (a) HOMO of the $[(\eta^5\text{-}C_5H_5)Re(NO)(PPh_3)]^+$ fragment, (b) idealized structures of Re=C geometric isomers of alkylidene complexes $[(\eta^5\text{-}C_5H_5)Re(NO)(PPh_3)(=CHR)]^+X^-$ (1^+X^-), and (c) idealized structures of diastereomers of alkene complexes $[(\eta^5\text{-}C_5H_5)Re(NO)(PPh_3)(H_2C=CHR)]^+X^-$ (2^+X^-).

The preceding transformations are most frequently observed with positively charged complexes. Note that any charge is readily delocalized onto C_α of alkylidene and vinylidene complexes, as exemplified in resonance form C in eq i. Thus, these hydride migrations can be viewed as types of Wagner–Meerwein rearrangements. Also, there is a substantial contribution by metallacyclic resonance forms to the ground states of the π complexes, as illustrated by D in eq i.

We sought to probe the mechanism of eq i, where L_nM^{n+} is the chiral rhenium cation $[(\eta^5\text{-}C_5H_5)Re(NO)(PPh_3)]^+$ (I). The fragment I is a powerful π donor, with the high-lying d-orbital HOMO depicted in Figure 1a.[14] We have previously shown that the corresponding alkylidene complexes $[(\eta^5\text{-}C_5H_5)Re(NO)(PPh_3)(=CHR)]^+X^-$ (1^+X^-) are easily prepared as either of the two Re=C geometric isomers II and III (*sc*, *ac*), illustrated in Figure 1b.[15] In each case, overlap of the rhenium fragment HOMO with the =CHR ligand p-acceptor orbital is maximized. Equilibrium constants and interconversion rates have been measured for several complexes. Typically, $K_{eq}(ac/sc) = 9$–10 and $\Delta H^\ddagger$ ($sc \rightarrow ac$) = 18–21 kcal/mol. Alkylidene complexes 1^+X^- are easily prepared with a variety of types of deuterium labels (C_α, C_β, PPh_3, C_5H_5) and in optically active form.[15]

The corresponding monosubstituted alkene complexes $[(\eta^5\text{-}C_5H_5)Re(NO)(PPh_3)(H_2C=CHR)]^+X^-$ (2^+X^-) have also been independently synthesized and thoroughly characterized.[16] Two configurational diastereomers are possible, as illustrated in Figure 1c. These differ in the alkene enantioface bound to the rhenium. One diastereomer is considerably more stable than the other (K_{eq}(*RS,SR*/*RR,SS*) $\simeq$ 10–20), but equilibration requires extended periods at 95–100 °C.[17] Importantly, the six "vinylic" protons of the two diastereomers exhibit well-separated ^1H NMR resonances at 300 MHz, and assignments have been previously established.[16]

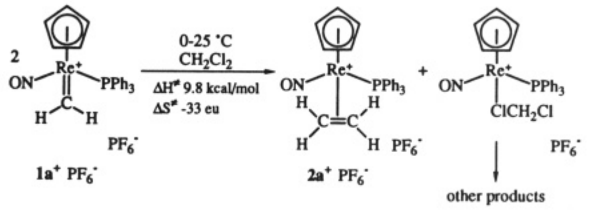

Figure 2. Thermolysis of methylidene complex $[(\eta^5\text{-}C_5H_5)Re(NO)(PPh_3)(=CH_2)]^+PF_6^-$ ($1a^+PF_6^-$).

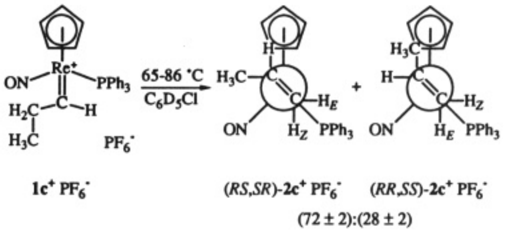

deuterium in reactant	deuterium in H_Z, H_E of product	
D_α ($Re=CDCH_2CH_3$)	40 ± 3 % H_Z 60 ± 3 % H_E	44 ± 3 % H_Z 56 ± 3 % H_E
2 D_β ($Re=CHCD_2CH_3$)	53 ± 3 % H_Z 47 ± 3 % H_E	40 ± 3 % H_Z 60 ± 3 % H_E

Figure 3. Thermolyses of propylidene complex $[(\eta^5\text{-}C_5H_5)Re(NO)(PPh_3)(=CHCH_2CH_3)]^+PF_6^-$ ($1c^+PF_6^-$) and deuterated derivatives.

In this paper, we describe an extensive mechanistic study of 1,2-hydride migrations in a series of rhenium alkylidene complexes 1^+X^-. A small portion of this work has been communicated.[6]

Results

1. Thermolysis of Methylidene and Ethylidene Complexes. The mechanism of decomposition of the methylidene complex $[(\eta^5\text{-}C_5H_5)Re(NO)(PPh_3)(=CH_2)]^+PF_6^-$ ($1a^+PF_6^-$) has been previously investigated in detail.[18] This compound cannot undergo a 1,2-hydride migration as in eq i. Instead, bimolecular coupling rapidly occurs above 0 °C to give the ethylene complex $[(\eta^5\text{-}C_5H_5)Re(NO)(PPh_3)(H_2C=CH_2)]^+PF_6^-$ ($2a^+PF_6^-$) and a solvate complex $[(\eta^5\text{-}C_5H_5)Re(NO)(PPh_3)(S)]^+PF_6^-$ (Figure 2). Thus, an analogous carbon–carbon bond forming process is potentially competitive with eq i in higher alkylidene complexes.

The ethylidene complex $[(\eta^5\text{-}C_5H_5)Re(NO)(PPh_3)(=CHCH_3)]^+PF_6^-$ ($1b^+PF_6^-$)[15b] was dissolved in C_6H_5Cl in an NMR tube.[19] The sample was heated and monitored by

---

[14] (a) Schilling, B. E. R.; Hoffmann, R.; Faller, J. W. *J. Am. Chem. Soc.* **1979**, *101*, 592. (b) Georgiou, S.; Gladysz, J. A. *Tetrahedron* **1986**, *42*, 1109.

[15] (a) Kiel, W. A.; Lin, G.-Y.; Constable, A. G.; McCormick, F. B.; Strouse, C. E.; Eisenstein, O.; Gladysz, J. A. *J. Am. Chem. Soc.* **1982**, *104*, 4865. (b) Kiel, W. A.; Lin, G.-Y.; Bodner, G. S.; Gladysz, J. A. *Ibid.* **1983**, *105*, 4958. (c) Kiel, W. A.; Buhro, W. E.; Gladysz, J. A. *Organometallics* **1984**, *3*, 879. (d) O'Connor, E. J.; Kobayashi, M.; Floss, H. G.; Gladysz, J. A. *J. Am. Chem. Soc.* **1987**, *109*, 4837. (e) Peng, T.-S.; Gladysz, J. A. *Organometallics* **1990**, *9*, 2884. (f) Kowalczyk, J. J.; Arif, A. M.; Gladysz, J. A. *Chem. Ber.* **1991**, *124*, 729.

[16] Bodner, G. S.; Peng, T.-S.; Arif, A. M.; Gladysz, J. A. *Organometallics* **1990**, *9*, 1191.

[17] Peng, T.-S.; Gladysz, J. A. *J. Chem. Soc., Chem. Commun.* **1990**, 902.

[18] Merrifield, J. H.; Lin, G.-Y.; Kiel, W. A.; Gladysz, J. A. *J. Am. Chem. Soc.* **1983**, *105*, 5811.

[19] Samples of ethylidene complex $1b^+PF_6^-$ contained small amounts of ethylene complex $2a^+PF_6^-$, and samples of propylidene complex $1c^+PF_6^-$ contained small amounts of propene complex $2c^+PF_6^-$. See the Discussion and Figure 12 for details.

^{31}P NMR. Complex **1b**$^+$PF$_6^-$ disappeared with a $t_{1/2} \approx 4$ h at 85 °C or 1 h at 110 °C. At least nine compounds formed. The major product (19.3 ppm) accounted for only 30% of the total area of the PPh$_3$ ^{31}P NMR resonances. An authentic sample of the coupling product, *cis*-2-butene complex $[(\eta^5\text{-C}_5\text{H}_5)\text{Re(NO)(PPh}_3)(\text{CH}_3\text{CH}{=}\text{CHCH}_3)]^+\text{BF}_4^-$, has been independently prepared and exhibits a ^{31}P NMR resonance at 7.7 ppm (C$_6$H$_5$Cl).[20] This complex constituted at most 14% of the product mixture.

2. Thermolysis of Propylidene and Pentylidene Complexes. Next, C$_6$D$_5$Cl solutions of propylidene complex $[(\eta^5\text{-C}_5\text{H}_5)\text{Re(NO)(PPh}_3)({=}\text{CHCH}_2\text{CH}_3)]^+\text{PF}_6^-$ (**1c**$^+$PF$_6^-$)[15b] were kept at 65–86 °C.[19] The Re=C isomer ratio (*ac*/*sc* = (91 ± 2)/(9 ± 2)) was unaffected, as assayed by ^{1}H NMR. Clean rearrangement to the diastereomeric propene complexes $[(\eta^5\text{-C}_5\text{H}_5)\text{Re(NO)(PPh}_3)(\text{H}_2\text{C}{=}\text{CHCH}_3)]^+\text{PF}_6^-$ (**2c**$^+$PF$_6^-$; Figure 3)[16,21] occurred over the course of several hours. Importantly, *non*equilibrium mixtures of diastereomers formed. In each case, *RS*,*SR*/*RR*,*SS* = (72 ± 2)/(28 ± 2) through 2.0–2.5$t_{1/2}$. When a C$_6$D$_5$Cl solution of **2c**$^+$PF$_6^-$ is kept at 95–100 °C for 16 h, a ca. 95/5 mixture of *RS*,*SR*/*RR*,*SS* diastereomers forms.[16]

Rates of the preceding reactions were measured by ^{1}H NMR as described in the Experimental Section. Isomerization was first order, and k_{obs} are summarized in entries 1–8 of Table I. All data are for the *sum* of the disappearance of the two Re=C isomers of **1c**$^+$PF$_6^-$ and/or the sum of the appearance of the two diastereomers of **2c**$^+$PF$_6^-$.[21] An Eyring plot gave $\Delta H^\ddagger = 27 \pm 1$ kcal/mol and $\Delta S^\ddagger = 3 \pm 3$ eu.[22] Both of these values are much more positive than those obtained for the bimolecular reaction in Figure 2.

Interestingly, **1c**$^+$PF$_6^-$ also cleanly isomerized to **2c**$^+$PF$_6^-$ over the course of 48 h at 65 °C in the solid state: *RS*,*SR*/*RR*,*SS* = (67 ± 2)/(33 ± 2).

The α-deuterated propylidene complex $[(\eta^5\text{-C}_5\text{H}_5)\text{Re(NO)(PPh}_3)({=}\text{CDCH}_2\text{CH}_3)]^+\text{PF}_6^-$ (**1c**$^+$-α-d_1-PF$_6^-$) was prepared as described previously.[15b] The rate of rearrangement to deuteriopropene complex $[(\eta^5\text{-C}_5\text{H}_5)\text{Re(NO)(PPh}_3)(\text{HDC}{=}\text{CHCH}_3)]^+\text{PF}_6^-$ (**2c**$^+$-d_1-PF$_6^-$) was similarly measured at 65–85 °C, as summarized in entries 9–13 of Table I. At all temperatures, **1c**$^+$-α-d_1-PF$_6^-$ decomposed *faster* than **1c**$^+$PF$_6^-$. The secondary kinetic deuterium isotope effect, $k_{\text{H}}/k_{\text{D}}$, was 0.50 at 65 °C and 0.58 at 85 °C.[23] Such *inverse* isotope effects are frequently observed when the deuterium is attached to a carbon that undergoes an sp^2 → sp^3 hybridization change.[24]

The diastereomers of **2c**$^+$-d_1-PF$_6^-$ formed in the preceding experiments were carefully analyzed by ^{1}H NMR. As summarized in Figure 3, deuterium was incorporated nearly equally into each of the geminal protons (H$_Z$/H$_E$ = (40 ± 3)/(60 ± 3)) in the *RS*,*SR* diastereomer. A similar distribution was found in the *RR*,*SS* diastereomer (H$_Z$/H$_E$ = (44 ± 3)/(56 ± 3)). Experiments reported elswhere establish that H$_Z$ and H$_E$ do not independently exchange in alkene complexes **2**$^+$X$^-$.[17] Thus, the rearrangement of **2c**$^+$PF$_6^-$ is not stereoselective at the migration terminus.

Table I. Rates of Rearrangement of Alkylidene Complexes 1$^+$X$^-$ to Alkene Complexes 2$^+$X$^-$

entry	complex (solvent)	temp (°C)	k_{obs} (s^{-1})
1	**1c**$^+$PF$_6^-$ (C$_6$D$_5$Cl)	65	$(4.31 \pm 0.06) \times 10^{-5}$
2		69	$(7.69 \pm 0.20) \times 10^{-5}$
3		73	$(2.05 \pm 0.07) \times 10^{-4}$
4		76	$(1.47 \pm 0.02) \times 10^{-4}$
5		78	$(3.30 \pm 0.13) \times 10^{-4}$
6		79	$(3.64 \pm 0.14) \times 10^{-4}$
7		85	$(4.57 \pm 0.05) \times 10^{-4}$
8		86	$(5.16 \pm 0.25) \times 10^{-4}$
	$\Delta H^\ddagger = 27 \pm 1$ kcal mol^{-1}; $\Delta S^\ddagger = 3 \pm 3$ eu		
9	**1c**$^+$-α-d_1-PF$_6^-$ (C$_6$D$_5$Cl)	65	$(1.01 \pm 0.02) \times 10^{-4}$
10		70	$(1.98 \pm 0.10) \times 10^{-4}$
11		75	$(3.62 \pm 0.18) \times 10^{-4}$
12		80	$(4.47 \pm 0.08) \times 10^{-4}$
13		85	$(1.03 \pm 0.06) \times 10^{-3}$
	$\Delta H^\ddagger = 26 \pm 1$ kcal mol^{-1}; $\Delta S^\ddagger = -1 \pm 3$ eu		
14	**1c**-β-d_2-PF$_6^-$ (C$_6$D$_5$Cl)	65	$(1.93 \pm 0.03) \times 10^{-5}$
15		70	$(9.06 \pm 0.30) \times 10^{-5}$
16		75	$(1.00 \pm 0.05) \times 10^{-4}$
17		80	$(2.12 \pm 0.08) \times 10^{-4}$
18		85	$(3.56 \pm 0.26) \times 10^{-4}$
	$\Delta H^\ddagger = 31 \pm 2$ kcal mol^{-1}; $\Delta S^\ddagger = 14 \pm 5$ eu		
19	**1c**$^+$-d_{18}-PF$_6^-$ (C$_6$D$_5$Cl)	65	$(4.54 \pm 0.12) \times 10^{-5}$
20	(–)-(*S*)-**1c**$^+$-PF$_6^-$ (C$_6$D$_5$Cl)	71	$(1.20 \pm 0.10) \times 10^{-4}$
21	**1d**$^+$PF$_6^-$ (C$_6$D$_5$Cl)	71	$(6.34 \pm 0.08) \times 10^{-5}$
22		77	$(1.02 \pm 0.14) \times 10^{-4}$
23		86	$(3.92 \pm 0.11) \times 10^{-4}$
24		90	$(6.89 \pm 0.24) \times 10^{-4}$
	$\Delta H^\ddagger = 31 \pm 4$ kcal mol^{-1}; $\Delta S^\ddagger = 13 \pm 8$ eu		
25	**1e**$^+$SO$_3$F$^-$ (CD$_2$Cl$_2$)	3	$(7.90 \pm 0.09) \times 10^{-5}$
26		15	$(4.55 \pm 0.19) \times 10^{-4}$
27		20	$(8.27 \pm 0.17) \times 10^{-4}$
28		25	$(1.28 \pm 0.06) \times 10^{-3}$
	$\Delta H^\ddagger = 21 \pm 1$ kcal mol^{-1}; $\Delta S^\ddagger = -3 \pm 3$ eu		
29	**1f**$^+$BF$_4^-$ (C$_6$H$_5$Cl)	82	$(3.32 \pm 0.24) \times 10^{-5}$
30		87	$(5.88 \pm 0.45) \times 10^{-5}$
31		92	$(1.11 \pm 0.08) \times 10^{-4}$
32		97	$(2.28 \pm 0.17) \times 10^{-4}$
	$\Delta H^\ddagger = 33 \pm 3$ kcal mol^{-1}; $\Delta S^\ddagger = 13 \pm 8$ eu		

Next, the β-dideuterated propylidene complex $[(\eta^5\text{-C}_5\text{H}_5)\text{Re(NO)(PPh}_3)({=}\text{CHCD}_2\text{CH}_3)]^+\text{PF}_6^-$ (**1c**$^+$-β-d_2-PF$_6^-$) was prepared as described previously.[15b] The rate of rearrangement to dideuteriopropene complex $[(\eta^5\text{-C}_5\text{H}_5)\text{Re(NO)(PPh}_3)(\text{HDC}{=}\text{CDCH}_3)]^+\text{PF}_6^-$ (**2c**$^+$-d_2-PF$_6^-$) was measured at 65–85 °C, as summarized in entries 14–18 of Table I. At all temperatures, **1c**$^+$-β-d_2-PF$_6^-$ decomposed *slower* than **1c**$^+$PF$_6^-$. The primary kinetic deuterium isotope effect, $k_{\text{H}}/k_{\text{D}}$, was 1.94 at 65 °C and 1.40 at 85 °C.[23,25] The location of deuterium in the product **2c**$^+$-d_2-PF$_6^-$ was analyzed as above. In each diastereomer, deuterium was distributed nearly equally between H$_Z$ and H$_E$, as summarized in Figure 3.

Additional types of experiments were conducted to further define the hydride migration mechanism. For example, phosphine ligand dissociation is a common elementary step. In principle, this can be probed by rate

---

[20] Pu, J.; Peng, T.-S. Unpublished results, University of Utah. The corresponding *trans*-2-butene complex has also been prepared. ^{31}P NMR (C$_6$H$_5$Cl, ppm): more stable diastereomer, 7.1; less stable, 7.9. The more stable diastereomer constituted at most 2% of the **1b**$^+$PF$_6^-$ thermolysis products.

[21] Importantly, the rearrangement of **1c**$^+$PF$_6^-$ to **2c**$^+$PF$_6^-$ is spectroscopically and preparatively quantitative, as ascertained by ^{1}H NMR experiments in the presence of an internal standard, and isolated product yields of >99% (Experimental Section).

[22] Standard deviations of $\Delta H^\ddagger$ and $\Delta S^\ddagger$ values (Table I) were estimated according to: Wiberg, K. B. *Physical Organic Chemistry*; Wiley: New York, 1964; pp 378–379. Isomerization rates were measured over 2.0–3.0$t_{1/2}$. Error limits given for individual rate constants are the standard deviations on the slopes of ln [C] vs t plots.

[23] Isotope effects were calculated from the least-squares fit of the Eyring data and differ slightly from those obtained from the ratios of the rate constants in Table I.

[24] (a) Haveli, E. A. *Prog. Phys. Org. Chem.* **1963**, *1*, 109. (b) Gajewski, J. J.; Hawkins, C. M.; Jimenez, J. L. *J. Org. Chem.* **1990**, *55*, 674 and references therein.

[25] Note that the second, nonmigrating deuterium contributes a secondary deuterium isotope effect (presumably small) to this $k_{\text{H}}/k_{\text{D}}$.

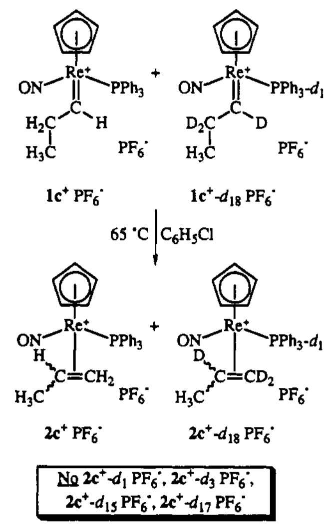

Figure 4. Cothermolysis of propylidene complexes $1c^+PF_6^-$ and $1c^+\text{-}d_{18}\text{-}PF_6^-$.

studies or exchange experiments using a labeled phosphine. However, phosphines reversibly add to the electrophilic alkylidene carbon of complexes 1^+X^- to give phosphonium salts $[(\eta^5\text{-}C_5H_5)Re(NO)(PPh_3)(CHRPR_3)]^+X^-$.[15a,b,26] Thus, we sought to test for phosphine dissociation via a crossover experiment.

First, the highly deuterated propylidene complex $[(\eta^5\text{-}C_5H_5)Re(NO)(PPh_3\text{-}d_{15})({=}CDCD_2CH_3)]^+PF_6^-$ ($1c^+\text{-}d_{18}\text{-}PF_6^-$) was prepared as desribed in the Experimental Section. The rate of rearrangement to deuteriopropene complex $[(\eta^5\text{-}C_5H_5)Re(NO)(PPh_3\text{-}d_{15})(D_2C{=}CDCH_3)]^+PF_6^-$ ($2c^+\text{-}d_{18}\text{-}PF_6^-$) was measured at 65 °C (entry 19, Table I) and found to be essentially equal to that of natural-abundance $1c^+PF_6^-$ (entry 1). Hence, the primary and inverse secondary kinetic deuterium isotope effects approximately cancel.

Next, equimolar amounts of $1c^+PF_6^-$ and $1c^+\text{-}d_{18}\text{-}PF_6^-$ were codecomposed in C_6H_5Cl (0.015 M) at 65 °C (Figure 4). The FAB mass spectrum of the resulting propene complex $2c^+\text{-}d_x\text{-}PF_6^-$ clearly showed crossover products to be absent. If phosphine dissociation occurred at any time on the reaction coordinate, $2c^+\text{-}d_3\text{-}PF_6^-$ and $2c^+\text{-}d_{15}\text{-}PF_6^-$ would have formed. Perhaps more importantly, this experiment also shows that hydride migrates intramolecularly. Otherwise, $2c^+\text{-}d_1\text{-}PF_6^-$ and $2c^+\text{-}d_{17}\text{-}PF_6^-$ would have been observed.

The optically active propylidene complex (−)-(*R*)-$1c^+PF_6^-$ was prepared from the optically active methyl complex (−)-(*R*)-$(\eta^5\text{-}C_5H_5)Re(NO)(PPh_3)(CH_3)$[27] by a procedure analogous to that employed for the racemate. Analysis with the chiral NMR shift reagent (+)-Eu(hfc)$_3$ showed the optical purity of (−)-(*R*)-$1c^+PF_6^-$ to be >96% ee.[19] The rate of rearrangement to the optically active propene complex (−)-$2c^+PF_6^-$ was measured at 71 °C and was close to that extrapolated for the racemate at that temperature ($1.11 \times 10^{-4}\ s^{-1}$). Chiral shift reagent analysis showed both product diastereomers to be of >98% ee. Comparison to an authentic sample of the enantiomeric salt (+)-$2c^+BF_4^-$ (mixture of *SR* and *SS* diastereomers)[16] established *retention* of configuration at rhenium.

Similar experiments were conducted with the pentylidene complex $[(\eta^5\text{-}C_5H_5)Re(NO)(PPh_3)({=}CHCH_2CH_2CH_2CH_3)]^+PF_6^-$ ($1d^+PF_6^-$). Clean rearrangement to the pentene complex $[(\eta^5\text{-}C_5H_5)Re(NO)(PPh_3)(H_2C{=}CHCH_2CH_2CH_3)]^+PF_6^-$ occurred (*RS*,*SR*/*RR*,*SS* = (66 ± 2):(34 ± 2)), as assayed by ^1H NMR. Rates were very slightly slower than those of $1c^+PF_6^-$, as summarized in entries 21–24 of Table I. An Eyring plot gave $\Delta H^\ddagger = 31 \pm 4$ kcal/mol and $\Delta S^\ddagger = 13 \pm 10$ eu.[22]

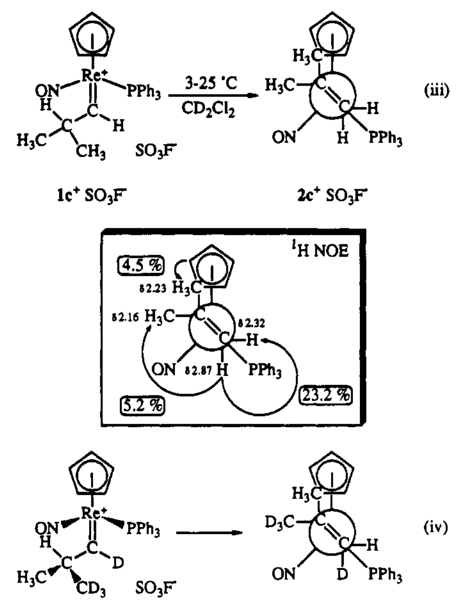

Figure 5. Thermolyses of isobutylidene complex $[(\eta^5\text{-}C_5H_5)Re(NO)(PPh_3)({=}CHCH(CH_3)_2)]^+SO_3F^-$ ($1e^+SO_3F^-$) and deuterated derivatives; data from ^1H difference NOE experiments.

3. Thermolysis of an Isobutylidene Complex. The isobutylidene complex $[(\eta^5\text{-}C_5H_5)Re(NO)(PPh_3)({=}CHCH(CH_3)_2)]^+SO_3F^-$ ($1e^+SO_3F^-$)[28] was studied next. Note that hydride migration originates at a tertiary carbon in $1e^+SO_3F^-$. Accordingly, rearrangement to isobutylene complex $[(\eta^5\text{-}C_5H_5)Re(NO)(PPh_3)(H_2C{=}C(CH_3)_2)]^+SO_3F^-$ ($2e^+SO_3F^-$)[16,28] occurred rapidly in CD_2Cl_2 at room temperature, as shown in Figure 5. Rates were measured by ^1H NMR at 3–25 °C, as summarized in entries 25–28 of Table I. These data gave $\Delta H^\ddagger = 21 \pm 1$ kcal/mol and $\Delta S^\ddagger = -3 \pm 3$ eu.[22]

As a prelude to deuterium labeling experiments, we sought to assign the "allylic" and "vinylic" ^1H NMR resonances of isobutylene complex $2e^+SO_3F^-$. Difference ^1H NOE experiments[29] have been previously conducted with a variety of alkene complexes 2^+X^-.[15f,16] Cyclopentadienyl ligand irradiation enhances the resonances of groups that are syn to the cyclopentadienyl ligand on the C=C carbon anti to the PPh_3 ligand. An analogous experiment with $2e^+BF_4^-$ enhanced only the downfield allylic methyl resonance (δ 2.23, 4.5%). Accordingly, this was assigned to the methyl group syn to the cyclopentadienyl ligand, as illustrated in Figure 5.

The downfield vinylic ^1H NMR resonance of $2e^+BF_4^-$ (δ 2.87) was subsequently irradiated. The upfield allylic methyl resonance (δ 2.16) exhibited an enhancement (5.2%), but the downfield methyl resonance (δ 2.23) was unaffected. Thus, the downfield vinylic proton was assigned as cis to the upfield allylic methyl group, as shown in Figure 5. The upfield vinylic proton resonance (δ 2.32)

---

[26] Crocco, G. L.; Lee, K. E.; Gladysz, J. A. *Organometallics* **1990**, *9*, 2819.

[27] Merrifield, J. H.; Strouse, C. E.; Gladysz, J. A. *Organometallics* **1982**, *1*, 1204.

[28] Bodner, G. S.; Smith, D. E.; Hatton, W. G.; Heah, P. C.; Georgiou, S.; Rheingold, A. L.; Geib, S. J.; Hutchinson, J. P.; Gladysz, J. A. *J. Am. Chem. Soc.* **1987**, *109*, 7688.

[29] Neuhaus, D.; Williamson, M. *The Nuclear Overhauser Effect in Structural and Conformational Analyses*; VCH: New York, 1989; Chapter 7.

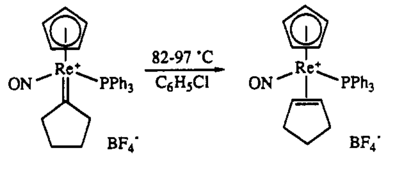

$1f^+ BF_4^-$ $2f^+ BF_4^-$

Figure 6. Thermolysis of cyclopentylidene complex $[(\eta^5\text{-}C_5H_5)Re(NO)(PPh_3)({=}C(CH_2)_4)]^+BF_4^-$ ($1f^+BF_4^-$).

was also enhanced (23.2%) in this experiment.[30]

Next, the stereochemistry of the rearrangement of deuterated $1e^+SO_3F^-$ was examined.

First, isomerization of the α-deuterated complex $[(\eta^5\text{-}C_5H_5)Re(NO)(PPh_3)({=}CDCH(CH_3)_2)]^+SO_3F^-$ ($1e^+$-α-d_1-SO_3F^-)[28] gave deuterioisobutylene complex $[(\eta^5\text{-}C_5H_5)Re(NO)(PPh_3)(HDC{=}C(CH_3)_2)]^+SO_3F^-$ ($2e^+$-d_1-SO_3F^-). Analysis by ^1H NMR showed 91 ± 5% of the deuterium to be in the site of the *down*field vinylic proton (δ 2.87). Thus, the rearrangement of $1e^+SO_3F^-$ is highly stereoselective at the migration terminus.

Second, rearrangement of the stereoselectively labeled trideuteriomethyl complex (*SS,RR*)-$[(\eta^5\text{-}C_5H_5)Re(NO)(PPh_3)({=}CHCH(CH_3)CD_3)]^+SO_3F^-$ ((*SS,RR*)-$1e^+$-γ-d_3-SO_3F^-)[28,31] was examined. Trideuterioisobutylene complex $[(\eta^5\text{-}C_5H_5)Re(NO)(PPh_3)(H_2C{=}C(CH_3)CD_3)]^+SO_3F^-$ formed with 89 ± 3% of the deuterium in the site of the *up*field allylic methyl group (δ 2.16). Thus, the rearrangement of $1e^+SO_3F^-$ is highly stereoselective at the migration origin. The aggregate result of the two preceding experiments is shown in eq iv of Figure 5 and analyzed in the Discussion.

4. Thermolysis of a Cyclopentylidene Complex. The synthesis of the cyclopentylidene complex $[(\eta^5\text{-}C_5H_5)Re(NO)(PPh_3)({=}C(CH_2)_4)]^+BF_4^-$ ($1f^+BF_4^-$) has been recently described.[15f] Complex $1f^+BF_4^-$ is the first disubstituted alkylidene complex of rhenium fragment $[(\eta^5\text{-}C_5H_5)Re(NO)(PPh_3)]^+$ (I) to be accessed. Thus, we sought to compare its thermal chemistry to that of monosubstituted alkylidene complexes $1b$–e^+X^-.

Complex $1f^+BF_4^-$ cleanly rearranged to the cyclopentene complex $[(\eta^5\text{-}C_5H_5)Re(NO)(PPh_3)(CH{=}CHCH_2CH_2CH_2)]^+BF_4^-$ ($2f^+BF_4^-$)[15f] at 82-97 °C in C_6H_5Cl, as assayed by ^{31}P NMR (Figure 6). Product identity was confirmed by workup and comparison of the ^1H NMR spectrum to that of an authentic sample. Rate data are summarized in entries 29-32 of Table I. An Eyring plot gave $\Delta H^\ddagger$ = 33 ± 3 kcal/mol and $\Delta S^\ddagger$ = 13 ± 8 eu.[22]

At corresponding temperatures, the rate of rearrangement of $1f^+BF_4^-$ is ca. 10 times slower than that of propylidene complex $1c^+PF_6^-$. Also, the previous observation that the stability of $1f^+BF_4^-$ is much greater in $CDCl_3$ was confirmed (little reaction at 110 °C, sealed tube).[15f]

Discussion

1. Reactivity Trends. The rates of Wagner–Meerwein rearrangements and related 1,2-shifts are commonly enhanced by (a) carbocation-stabilizing substituents at the migration origin and (b) an increase in the electrophilicity of the migration terminus.[32] Parallel rate trends are evident in the rearrangements of alkylidene complexes 1^+X^- described above, as summarized in Table I.

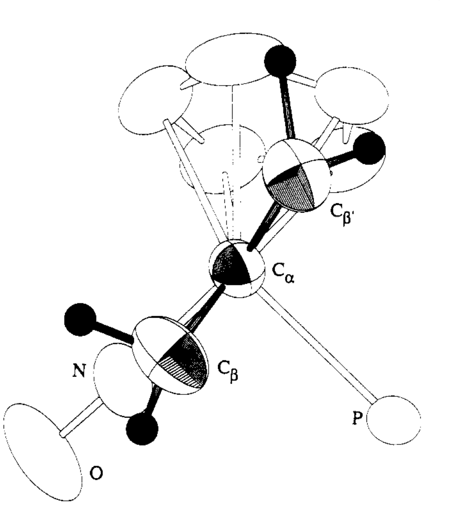

Figure 7. Partial structure of the cation of cyclopentylidene complex $[(\eta^5\text{-}C_5H_5)Re(NO)(PPh_3)({=}C(CH_2)_4]^+PF_6^-$. The PPh_3 phenyl rings and C_γ and $C_{\gamma'}$ of the cyclopentylidene ligand have been omitted.

For example, isobutylidene complex $1e^+SO_3F^-$, which has two carbocation-stabilizing methyl substituents at C_β, isomerizes the fastest. Propylidene complex $1c^+PF_6^-$ and pentylidene complex $1d^+PF_6^-$, which each have one C_β alkyl substituent, isomerize at much slower rates. Ethylidene complex $1b^+PF_6^-$, which lacks a C_β alkyl substituent, undergoes other thermolytic decomposition pathways.

Similar reactivity trends have been previously observed with other types of alkylidene complexes. For example, Brookhart has found that the iron ethylidene complex $[(\eta^5\text{-}C_5H_5)Fe(CO)(PPh_3)({=}CHCH_3)]^+CF_3SO_3^-$ decomposes with $t_{1/2} \approx$ 3 h at 25 °C.[1] The corresponding iron ethylene complex and other products form. However, the analogous iron propylidene complex $[(\eta^5\text{-}C_5H_5)Fe(CO)(PPh_3)({=}CHCH_2CH_3)]^+CF_3SO_3^-$ is less stable and cleanly isomerizes to a propene complex with $t_{1/2} \approx$ 1 h at -40 °C.

Note that these iron alkylidene complexes rearrange much faster than the "isoelectronic" rhenium analogues $1b,c^+PF_6^-$. This is most logically attributed to enhanced C_α electrophilicity. Thus, the iron fragment $[(\eta^5\text{-}C_5H_5)Fe(CO)(PPh_3)]^+$ must be a poorer π donor than the rhenium fragment $[(\eta^5\text{-}C_5H_5)Re(NO)(PPh_3)]^+$ (I). This conclusion is supported by a variety of other data.[13,33]

Cyclopentylidene complex $1f^+BF_4^-$ isomerizes more slowly than propylidene and pentylidene complexes $1c,d^+PF_6^-$. All three of these compounds bear one C_β alkyl substituent. Thus, we ascribe the greater stability of $1f^+BF_4^-$ to a decrease in C_α electrophilicity resulting from a second C_α alkyl substituent. Note also that, unlike $1c,d^+PF_6^-$, Re=C geometric isomers are not possible for $1f^+BF_4^-$. The crystal structure of the hexafluorophosphate salt $1f^+PF_6^-$ has been determined, and all cyclopentylidene ligand hydrogens have been located.[15f] As shown in Figure 7, the C_β hydrogens on the Re=C face *opposite* to the bulky PPh_3 ligand are best aligned for migration to C_α.

Casey has synthesized and studied the chemistry of the iron isopropylidene complex $[(\eta^5\text{-}C_5H_5)Fe(CO)(PPh_3)({=}C(CH_3)_2)]^+CF_3SO_3^-$, which also bears two C_α alkyl sub-

---

[30] A different assignment of resonances was proposed earlier.[6] Previous NOE experiments involved irradiation of the δ 2.23 resonance and likely employed too strong a decoupling power.

[31] The sample of (*SS,RR*)-$1e^+$-γ-d_3 utilized is a (92 ± 2)/(8 ± 2) mixture of *SS,RR* and *SR,RS* diastereomers.

[32] Schubin, V. G. In *Topics in Current Chemistry*; Rees, C., Ed.; Springer-Verlag: New York, 1984; 116/117, pp 267-341.

[33] Lichtenberger, D. L.; Rai-Chaudhuri, A.; Seidel, M. J.; Gladysz, J. A.; Agbossou, S. K.; Igau, A.; Winter, C. H. *Organometallics* **1991**, *10*, 1355.

stituents. Accordingly, it is more stable than the analogous iron ethylidene complex described above.[4] Rearrangement to the corresponding propene complex occurs with $t_{1/2} \approx$ 15 min at 45 °C.

2. Other Rate Considerations. Several additional aspects of the data in Table I merit analysis. However, it should be emphasized that all rate constants are calculated from the sum of the disappearance of *both* Re=C isomers. Thus, the k_{obs} and derived activation parameters do not represent properties of a single elementary reaction step.

Importantly, rearrangements of alkylidene complexes 1^+X^- generally occur under conditions where the interconversion of Re=C geometric isomers is rapid. Thus, the Curtin–Hammet principle[34] will apply, and reaction will occur predominantly via the Re=C isomer that gives the lower transition state energy. Only with isobutylidene complex $1e^+SO_3F^-$ is the $\Delta H^{\ddagger}$ (21 ± 1 kcal/mol) comparable to that expected for Re=C isomerization (18–21 kcal/mol). However, our NMR data clearly show that both Re=C isomers of $1e^+SO_3F^-$ simultaneously disappear under the thermolysis conditions. At this time, we see no reason to attribute any special *enhanced* reactivity to the less stable *sc* Re=C isomers. Thus, transition states derived from the more stable *ac* Re=C isomers are emphasized in the analyses below.

The modest primary kinetic isotope effects obtained with $1c^+$-β-d_2-PF_6^- vary slightly with temperature (1.94–1.40)[23] and are in a typical range for 1,2-hydride migrations.[35] The low values are logically ascribed to enforced nonlinear transition states.[36] Interestingly, a plot of log (k_H/k_D) versus $1/T$ is linear. Such relationships have sometimes been analyzed in terms of transition-state structures.[37] However, the validity of such correlations has been questioned.[38]

The $\Delta H^{\ddagger}$ for the isomerizations of $1c^+$-β-d_2-PF_6^- and $1c^+$-α-d_1-PF_6^- (Table I) deviate in the expected directions from that of $1c^+PF_6^-$. However, the $\Delta S^{\ddagger}$ also vary noticeably. Furthermore, neglecting the often appreciable error limits,[22] there is roughly parallel increase in $\Delta S^{\ddagger}$ with $\Delta H^{\ddagger}$ for all of the substrates in Table I. Such behavior constitutes an "isokinetic relationship" and is often taken as evidence for a common rate-determining step.[39]

3. Stereochemistry of Hydride Migration. Wagner–Meerwein rearrangements and related 1,2-sigmatropic shifts are commonly analyzed as two-electron transition states. However, the isomerization of an alkylidene complex to an alkene complex (eq i) can be viewed as a four-electron process involving two electrons from a carbon–hydrogen σ bond and two electrons from a rhenium–carbon π bond. These correlate to vinylic carbon–hydrogen and rhenium–carbon σ bonds in the metallacyclopropane-like product.[40] Concerted rearrangements that proceed by four-electron transition states are often highly stereoselective.[41]

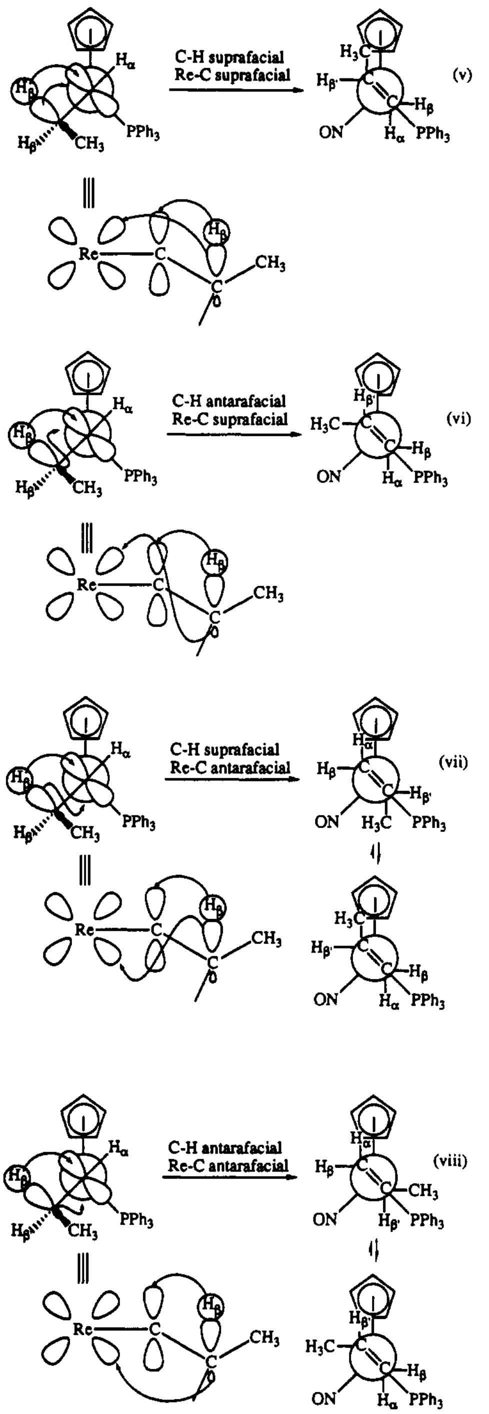

Figure 8. Some possible transition states for rearrangement of propylidene complex $1c^+PF_6^-$ to propene complex $2c^+PF_6^-$.

Some possible hydride migration transition states for propylidene complex $1c^+PF_6^-$ are sketched in Figure 8. In order to simply the initial analysis, two arbitrary restrictions are imposed: (1) Only the more stable *ac* Re=C geometric isomer is considered (see above), and (2) only transition states in which hydride migrates along the alkylidene face opposite to the bulky PPh_3 ligand are shown. The latter is consistent with the geometric bias in Figure

---

(34) Seeman, J. I. *Chem. Rev.* **1983**, *83*, 83.

(35) (a) Drewello, T.; Burgers, P. C.; Zummack, W.; Apeloig, Y.; Schwarz, H. *Organometallics* **1990**, *9*, 1161. (b) See also: Shriner, V. J., Jr.; Jewett, J. G. *J. Am. Chem. Soc.* **1965**, *87*, 1382.

(36) Lowry, T. H.; Richardson, K. S. *Mechanism and Theory in Organic Chemistry*, 3rd ed.; Harper and Row: New York, 1987; pp 236–237.

(37) Kwart, H. *Acc. Chem. Res.* **1982**, *15*, 401.

(38) (a) McLennan, D. J.; Gill, P. M. W. *J. Am. Chem. Soc.* **1985**, *107*, 2971. (b) Anhede, B.; Bergman, N.-A. *Ibid.* **1984**, *106*, 7634.

(39) (a) Linert, W.; Jameson, R. F. *Chem. Soc. Rev.* **1989**, *18*, 477. (b) Giese, B. *Acc. Chem. Res.* **1984**, *17*, 438. (c) Linert, W. *Inorg. Chim. Acta* **1988**, *141*, 233.

(40) Other, more complex, transition states can be formulated. For example, involvement of the rhenium fragment SHOMO (which is orthogonal to HOMO I and back-bonds into the NO ligand) to give a six-electron transition state might be invoked. This would initially produce alkene complexes in which the Re–(C=C) conformations are orthogonal to those shown in Figure 1.

(41) For example, the electrocyclic ring opening of aziridines and related three-membered-ring compounds to 1,3-dipoles is stereospecific. Huisgen, R. In *1,3-Dipolar Cycloaddition Chemistry*; Padwa, A., Ed.; Wiley: New York, 1984; Vol. 1, pp 20–21, 23–24, 74–75.

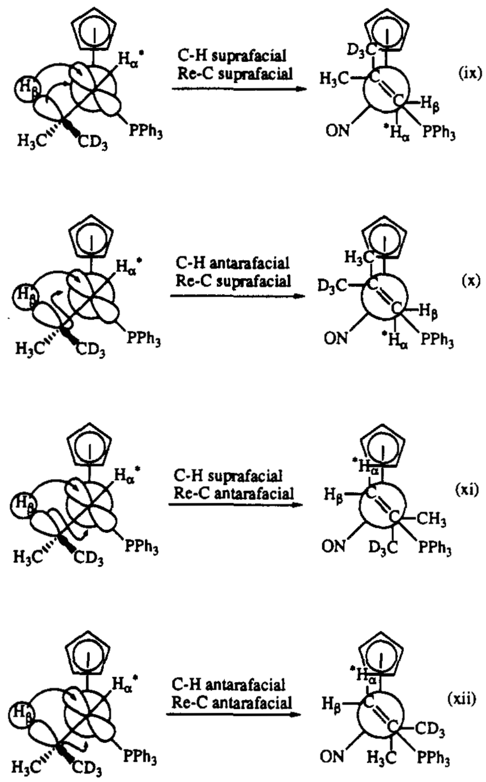

Figure 9. Some possible transition states for rearrangement of isobutylidene complex $1e^+$-d_n-SO_3F^- to isobutylene complex $2e^+$-d_n-SO_3F^-.

7 and the dominant direction of nucleophilic attack upon C_α of these alkylidene complexes.[15a-d]

In eqs v and vi of Figure 8, the Re═C π bond of $1c^+PF_6^-$ is broken suprafacially. The propylidene ligand C_α moves closer to the PPh_3 ligand as the reaction coordinate progresses. At the same time, C_β pivots about C_α and assumes the C═C position anti to the PPh_3 ligand in the product, propene complex $2c^+PF_6^-$.

Next, consider the carbon–hydrogen bond in eqs v and vi of Figure 8. It is easily seen that suprafacial cleavage (eq v) gives one diastereomer of propene complex $2c^+PF_6^-$, whereas antarafacial cleavage (eq vi) gives the other. Finally, there are two complementary transition states in which the Re═C π bond participates in an antarafacial manner (eqs vii and viii, Figure 8). Each of these initially give the propene ligand in its less stable Re—($C\frown C$) rotamer,[16] with the substituted carbon syn to the bulky PPh_3 ligand. However, the label patterns (H_α, H_β, $H_{\beta'}$) are identical with those obtained in eqs v and vi.

The transition states illustrated in eqs vi and vii are of "Mobius" geometry and hence are "symmetry allowed". They constitute plausible pathways to each of the observed diastereomers of $2c^+PF_6^-$. However, they also lead to the prediction that rearrangement of deuterated propylidene complexes $1c^+$-α-d_1-PF_6^- and $1c^+$-β-d_2-PF_6^- should give a specific label pattern in each product diastereomer. The fact that mixtures of deuterated isomers are obtained (Figure 3) requires that additional transition states are operative.

There are numerous possibilities for competing transition states. For example, all of the equations in Figure 8 have variants in which a rotamer of the C_α–C_β bond of $1c^+PF_6^-$ is employed. These are depicted in Figure 8b of the supplementary material. Consider a 120° clockwise rotation of C_β in eq vi. This moves the methyl group into the position formerly held by $H_{\beta'}$, with the result that the *less* stable diasteromer of $2c^+PF_6^-$ is now produced, but with $H_{\beta'}$ cis to the methyl group. This differs from the label pattern produced via eq vii or v.[42]

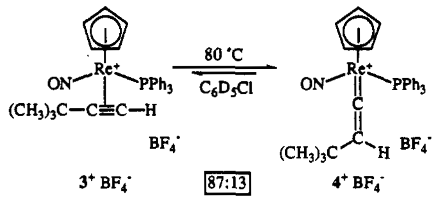

Figure 10. Thermolysis of *tert*-butylacetylene complex $[(\eta^5\text{-}C_5H_5)Re(NO)(PPh_3)(HC{\equiv}CC(CH_3)_3)]^+BF_4^-$ ($3^+BF_4^-$).

In contrast to $1c^+PF_6^-$, the isomerization of $1e^+SO_3F^-$ is highly stereoselective at both the migration origin and terminus. Thus, fewer competing transition states are available. Figure 9 illustrates four possible pathways that are analogous to those in Figure 8. Note that there can be only one reactive C_α–C_β rotamer of $1e^+SO_3F^-$ if hydride migration is restricted to the alkylidene face opposite the PPh_3 ligand.

The transition states shown in eqs x and xi are symmetry allowed. However, only the former gives the correct stereochemistry in the product $2e^+$-d_n-SO_3F^-. The latter initially yields $2e^+SO_3F^-$ with the two methyl groups on the C═C carbon syn to the bulky PPh_3 ligand—a much less stable Re–($C\frown C$) rotamer than is produced in eq x. The experimentally observed label pattern is also generated in eq xii. However, this symmetry-forbidden transition state also gives the less stable product Re—($C\frown C$) rotamer and is unlikely to be competitive with eq x.

Similar analyses have been conducted for transition states analogous to those in Figure 9, but involving (1) the less stable *sc* isomer of $1e^+SO_3F^-$ and (2) hydride migration along the alkylidene face syn to the PPh_3 ligand. These are illustrated in Figure 9b,c of the supplementary material. *In neither case is the experimentally observed product stereochemistry reproduced.* Thus, within this simple four-electron mechanistic construct, the transition state for isomerization of $1e^+SO_3F^-$ appears to be uniquely defined.

4. Related Chemistry. We have recently found that the isomerization of terminal alkyne to vinylidene ligands (eq ii) can also be observed with this class of rhenium complexes. Thus, thermolysis of the *tert*-butylacetylene complex $[(\eta^5\text{-}C_5H_5)Re(NO)(PPh_3)(HC{\equiv}CC(CH_3)_3)]^+BF_4^-$ ($3^+BF_4^-$) at 60–80 °C gives the *tert*-butylvinylidene complex $[(\eta^5\text{-}C_5H_5)Re(NO)(PPh_3)({=}C{=}CHC(CH_3)_3)]^+BF_4^-$ ($4^+BF_4^-$) as shown in Figure 10. Importantly, the rearrangement proceeds only to ca. 87% completion, and an identical mixture forms upon heating pure $4^+BF_4^-$. This demonstrates that eq ii is a true reversible equilibrium. We suggest by analogy that eq i is similarly reversible, although the spontaneous isomerization of an alkene complex to an alkylidene has not to our knowledge been explicitly observed.

There is good evidence, particularly for coordinatively unsaturated complexes, that the isomerization of terminal alkyne ligands (eq ii) can proceed via sequential carbon–hydrogen bond oxidative addition and 1,2-hydride migration.[12b] Thus, another possible mechanism for eq i

---

[42] Importantly, transition states involving C_α–C_β rotamers of $1c^+PF_6^-$ cannot account for the scrambling of H_α into both geminal positions of $2c^+PF_6^-$ (Figure 3). However, if hydride migration can occur via the less stable *sc* Re═C isomer of $1c^+PF_6^-$, or along the alkylidene face syn to the PPh_3 ligand, the H_α label will scramble. These possibilities are diagrammed in Figure 8c,d of the supplementary material. Thus, exceptions to one of the two arbitrary premises utilized in Figure 8 can likely occur.

would entail a 1,3-hydride shift to give a vinyl hydride complex as shown in eq xiii,[43] followed by carbon–hydrogen

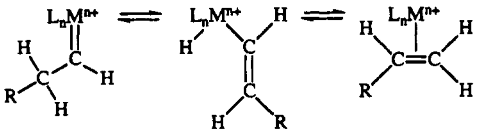

(xiii)

bond reductive elimination to give a coordinated alkene. Our data with complexes 1^+X^- do not appear to be consistent with this model. In particular, the marked inverse secondary kinetic deuterium isotope effect observed with $1c^+$-α-d_1-PF_6^- would require the second step to be rate determining. However, this would not rationalize the large rate accelerations found with carbocation-stabilizing C_β substituents or the rate retardations observed with carbocation-stabilizing C_α substituents.

Schrock has reported that the rearrangement of the *neutral* tungsten(IV) (or tungsten(VI)) ethylidene complex $W(OC(CH_3)_3)_2(O_2CPh)_2({=}CHCH_3)$ to the corresponding ethylene complex is catalyzed by benzoic acid.[7] High oxidation state alkylidene complexes are commonly nucleophilic at C_α. Accordingly, good evidence was obtained for initial C_α protonation to give an ethyl complex. However, such mechanisms are very unlikely to have analogy with low oxidation state, electrophilic alkylidene complexes 1^+X^-.[43]

We are not presently aware of a *purely organic* counterpart to eq i, or the reverse, that proceeds in a concerted fashion via a four-electron transition state. Apparently, cyclopropanes generally have lower energy thermolysis pathways available.[44] However, singlet carbenes often undergo facile hydride 1,2-migrations to give alkenes, as exemplified in eq xiv of Figure 11.[45] This constitutes an ametallic analogue of eq i. Also, Jones and co-workers have reported a *formal* 1,2-shift of an allylic hydride that results in cyclopropane ring formation, as illustrated in eq xv of Figure 11.[46]

The unbranched monosubstituted alkylidene complexes utilized in this work are prepared by reactions of the corresponding alkyl complexes $(\eta^5$-$C_5H_5)Re(NO)(PPh_3)(CH_2CH_2R)$ and $Ph_3C^+PF_6^-$. The regiochemistry of hydride abstraction from this class of alkyl complexes has been previously studied.[15b] For example, addition of $Ph_3C^+BF_4^-$ to the β-phenyl-substituted complex $(\eta^5$-$C_5H_5)Re(NO)(PPh_3)(CH_2CH_2C_6H_5)$ gives both α-hydride abstraction to an alkylidene complex (major, 63%) and β-hydride abstraction to an alkene complex (minor, 36%), as summarized in Figure 12. However, in the course of our preparative work we noticed small but significant amounts of β-hydride abstraction from the corresponding ethyl and propyl complexes. Examination of ^1H NMR spectra from earlier experiments showed the presence of corresponding amounts of the resulting alkene complexes. Thus, revised regiochemical data are given in Figure 12. An increase in the carbocation-stabilizing ability of the C_β substituents clearly leads to an increase in β-hydride abstraction.

5. Summary. The mechanism of isomerization of alkylidene complexes 1^+X^- to alkene complexes 2^+X^- has been probed by a large number of diverse experiments. These rearrangements are intramolecular, occur without PPh_3 ligand dissociation, and proceed with retention of configuration at rhenium. They exhibit many similarities to 1,2-hydride shifts or Wagner–Meerwein rearrangements of organic compounds (substituent effects, primary and secondary kinetic deuterium isotope effects). However, in contrast to organic reaction analogues, a minimum of four electrons are involved in the transition state. The highly stereoselective isomerization of isobutylidene complex $1e$-d_n^+-SO_3F^- allows a unique symmetry-allowed reaction pathway to be identified.

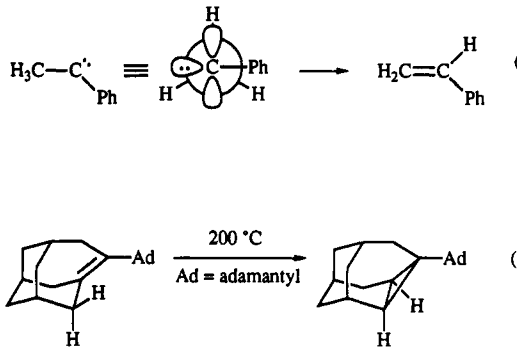

Figure 11. Some relevant organic hydride migrations.

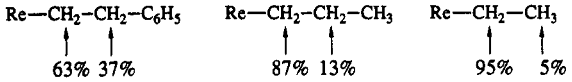

Figure 12. Revised regiochemical data for hydride abstraction $(Ph_3C^+X^-)$ from ethyl and propyl complexes $(\eta^5$-$C_5H_5)Re(NO)(PPh_3)(CH_2CH_2R)$.

Experimental Section

General Data. NMR spectra were recorded on Varian XL-300 spectrometers (^1H, referenced to $Si(CH_3)_4$ at δ 0.00; $^{31}P\{^1H\}$, referenced to external H_3PO_4 at 0.0 ppm). Mass spectra were obtained on a VG Micromass 7050-E double-focusing high-resolution mass spectrometer with a VG data system 2000. Optical rotations were measured on a Perkin-Elmer 241 MC polarimeter. Solvents and reagents were purified as follows: CH_2Cl_2, C_6H_5Cl, and $CHCl_3$, distilled from P_2O_5; CD_2Cl_2, vacuum transferred from CaH_2; C_6H_5Cl (Cambridge Isotopes), PPh_3-d_{15}, and (+)-Eu(hfc)$_3$ (Aldrich), used as received.

Syntheses of Deuterated Compounds. Complexes $[(\eta^5$-$C_5H_5)Re(NO)(PPh_3)({=}CDCH_2CH_3)]^+PF_6^-$ ($1c^+$-α-d_1-PF_6^-) and $[(\eta^5$-$C_5H_5)Re(NO)(PPh_3)({=}CHCD_2CH_3)]^+PF_6^-$ ($1c^+$-β-d_2-PF_6^-) were prepared as described previously.[15b] No residual protium was found by ^1H NMR (≥98% and ≥96% ^2H; integration vs C_5H_5 resonance). Complex $[(\eta^5$-$C_5H_5)Re(NO)(PPh_3$-$d_{15})({=}CDCD_2CH_3)]^+PF_6^-$ ($1c^+$-d_{18}-PF_6^-) was prepared from the precursor $[(\eta^5$-$C_5H_5)Re(NO)(PPh_3$-$d_{15})(CO)]^+BF_4^-$,[18] which was synthesized analogously to the undeuterated compound and then subjected to a combination of the steps used to obtain $1c^+$-α-d_1-PF_6^- and $1c^+$-β-d_2-PF_6^-. The deuteration level was assayed by mass spectrometry as described below. Deuterated isobutylidene complexes $[(\eta^5$-$C_5H_5)Re(NO)(PPh_3)({=}CHCH(CH_3)_2)]^+$-$d_n$-$SO_3F^-$ ($1e^+$-d_n-SO_3F^-) were generated as described previously.[28]

Representative Thermolyses. A. Under a N_2 atmosphere, a 5-mm NMR tube was charged with $1c^+PF_6^-$ (11.2 mg, 0.015 mmol)[15b] and C_6D_5Cl (0.4 mL) and capped with a septum. The tube was transferred to a NMR probe that had been preequilibrated to the appropriate temperature (Table I).[47] The dis-

---

[43] The C_β protons of alkylidene complexes 1^+X^- are quite acidic (appreciable abstraction occurs with the weak base $CHCl_2CO_2^-$ in CD_2Cl_2).[28] Thus, rearrangement mechanisms involving the ionization of H_β also deserve consideration. However, these would likely lead to crossover products such as $2c^+$-d_1-PF_6^- and $2c^+$-d_{17}-PF_6^- in Figure 4.

[44] But see Jug, K. *Theor. Chim. Acta.* **1976**, *42*, 303.

[45] Evanseck, J. D.; Houk, K. N. *J. Am. Chem. Soc.* **1990**, *112*, 9148 and references therein.

[46] Sellers, S. F.; Kleback, T. C.; Hollowood, F.; Jones, M., Jr.; Schleyer, P. v. R. *J. Am. Chem. Soc.* **1982**, *104*, 5492.

[47] For ^1H NMR rate experiments, probe temperatures were calibrated with either methanol or ethylene glycol standards: Van Geet, A. L. *Anal. Chem.* **1968**, *40*, 2227. For $^{31}P\{^1H\}$ NMR rate experiments ($1f^+BF_4^-$), a sealed capillary of ethylene glycol was inserted into the sample. After an equilibration period (to allow for any decoupler-induced heating), the observe nucleus was switched to ^1H and the temperature immediately calibrated as above. Corrections averaged 2 °C.

appearance of the $\mathrm{C_5H_5}$ and $\mathrm{CH_3}$ ^{1}H NMR resonances of both Re=C isomers of $\mathbf{1c}^+\mathrm{PF_6}^-$ ($\delta(ac)/\delta(sc)$ = 5.65/5.65, 0.70/0.65) and the appearance of the analogous resonances of both diastereomers of $\mathbf{2c}^+\mathrm{PF_6}^-$ ($\delta(RS,SR)/\delta(RR,SS)$ = 5.41/5.34, 1.85/1.97) were monitored. For each spectrum, areas of the cyclopentadienyl resonances were normalized to 100 (which equalizes disappearance and appearance rates).[21] The methyl resonances were treated analogously, and data from the two sets of resonances were averaged (agreement within 1%). Standard plotting procedures[48] gave the rates in Table I.

B. A 5-mm NMR tube was charged with $[(\eta^5\text{-}\mathrm{C_5H_5})\mathrm{Re(NO)(PPh_3)}(=\overline{\mathrm{C}(\mathrm{C}}\mathrm{H_2})_4)]^+\mathrm{BF_4}^-$ ($\mathbf{1f}^+\mathrm{BF_4}^-$;[15f] 6.7 mg, 0.0096 mmol) and $\mathrm{C_6H_5Cl}$ (0.5 mL) and capped with a septum. The sample was freeze–pump–thaw degassed three times. The tube was transferred to a NMR probe that had been preequilibrated to the appropriate temperature (Table I).[47] The disappearance of $\mathbf{1f}^+\mathrm{BF_4}^-$ and the appearance of $\mathbf{2f}^+\mathrm{BF_4}^-$ were monitorerd by ^{31}P NMR (14.6, 8.2 ppm). Rates were calculated as described in the preceding experiment.

Cothermolysis of $\mathbf{1c}^+\mathrm{PF_6}^-$ and $\mathbf{1c}^+\text{-}d_{18}\text{-}\mathrm{PF_6}^-$. Under a $\mathrm{N_2}$ atmosphere, a 5-mm NMR tube was charged with $\mathbf{1c}^+\mathrm{PF_6}^-$ (11.2 mg, 0.015 mmol), $\mathbf{1c}^+\text{-}d_{18}\text{-}\mathrm{PF_6}^-$ (11.4 mg, 0.015 mmol), and $\mathrm{C_6H_5Cl}$ (1 mL). The tube was kept at 85 °C for 5 h. The sample was then transferred to a flask, and solvent was removed by rotary evaporation. The residue was dissolved in $\mathrm{CHCl_3}$ (1 mL) and layered with hexane. The resulting precipitate was collected by filtration to give $\mathbf{2c}^+\text{-}d_x\text{-}\mathrm{PF_6}^-$ (22.4 mg, ca. 0.015 mmol) as a tan powder. Mass spectrum ((+)-FAB (7 kV, Ar, 3-nitrobenzyl alcohol/$\mathrm{CHCl_3}$): m/z (relative intensity)): $\mathbf{2c}^+\text{-}d_0\text{-}\mathrm{PF_6}^-$, 583/584/585/586/587 (4/61/23/100/27); $\mathbf{2c}^+\text{-}d_{18}\text{-}\mathrm{PF_6}^-$, 601/602/603/604/605 (5/58/25/100/26); precursor $\mathbf{1c}^+\text{-}\mathrm{PF_6}^-$, 583/584/585/586/587 (4/61/24/100/26); precursor $\mathbf{1c}^+\text{-}d_{18}\text{-}\mathrm{PF_6}^-$, 601/602/603/604/605 (5/60/26/100/28).

Synthesis and Thermolysis of (−)-(R)-$\mathbf{1c}^+\text{-}\mathrm{PF_6}^-$. A. Optically active methyl complex (−)-(R)-$(\eta^5\text{-}\mathrm{C_5H_5})\mathrm{Re(NO)(PPh_3)(CH_3)}$[18] was converted to optically active propyl complex (−)-(R)–$(\eta^5\text{-}\mathrm{C_5H_5})\mathrm{Re(NO)(PPh_3)(CH_2CH_2CH_3)}$ by a procedure analogous to that given for the racemate.[15b] This was in turn transformed to (−)-(R)-$\mathbf{1c}^+\mathrm{PF_6}^-$ ($[\alpha]^{25}_{589}$ −90.8° ± 3.2° (c 1.3 mg/mL, $\mathrm{CH_2Cl_2}$)) by a procedure analogous to that reported for the racemate.[15b] The chiral ^{1}H NMR shift reagent (+)-Eu(hfc)$_3$ gave near-base-line separation of the $\mathrm{C_5H_5}$ and $\mathrm{CH_3}$ resonances of racemic $\mathbf{1c}^+\mathrm{PF_6}^-$ ($\mathrm{CD_2Cl_2}$). An identical analysis of (−)-(R)-$\mathbf{1c}^+\mathrm{PF_6}^-$ established an enantiomeric excess of ≥96%. The sample contained ca. 13% of optically active propene complex (−)-$\mathbf{2c}^+\mathrm{PF_6}^-$ ((67 ± 3)/(33 ± 3) = SR/SS).[19] The enantiomeric tetrafluoroborate salt (+)-$\mathbf{2c}^+\mathrm{BF_4}^-$ has been previously characterized ($[\alpha]^{25}_{589}$ 115° ($\mathrm{CHCl_3}$), (67 ± 2)/(33 ± 2) = RS/RR).[16]

B. A Schlenk tube was charged with solid (−)-(R)-$\mathbf{1c}^+\mathrm{PF_6}^-$ (50 mg, 0.068 mmol) and kept at 65 °C for 48 h. Optically active (−)-$\mathbf{2c}^+\mathrm{PF_6}^-$ was recovered in quantitative yield ($[\alpha]^{25}_{589}$ −95.6° ± 2.3° (c 1.0 mg/mL, $\mathrm{CH_2Cl_2}$)).[49] A ^{1}H NMR spectrum ($\mathrm{CD_2Cl_2}$) showed a (67 ± 2)/(33 ± 2) ratio of SR and SS diastereomers, and addition of (+)-Eu(hfc)$_3$ established an enantiomeric excess of ≥98% for each diastereomer (base-line resonance separation).[16]

Representative ^{1}H NOED Experiment.[29] A 5-mm NMR tube was charged with $\mathbf{2e}^+\mathrm{BF_4}^-$ (11.5 mg, 0.017 mmol)[50] and $\mathrm{CD_2Cl_2}$ (0.5 mL) and capped with a septum. The sample was freeze–pump–thaw degassed three times. The NOE experiment was performed as an array consisting of two spectra each in which the first was obtained with 75% irradiation of the cyclopentadienyl resonance and the second with the decoupler frequency set >2 ppm from all resonances. Spectra were obtained at 23 °C in interleaved blocks of 32 transients with four steady states per block for a total of 1920 transients (acquisition time 2.0 s; pulse delay 8 s). The off-resonance spectrum was subtracted from the cyclopentadienyl-irradiated spectrum to give the difference NOE data.

Acknowledgment. We thank the DOE for support of this research.

Supplementary Material Available: Representative plots of rate data and mechanistic alternatives to Figures 8 and 9 (8 pages). Ordering information is given on any current masthead page.

---

(48) Espenson, J. H. *Chemical Kinetics and Reaction Mechanisms*; McGraw-Hill: New York, 1981; Chapter 2.

(49) If optically active $\mathbf{2c}^+\mathrm{BF_4}^-$ and $\mathbf{2c}^+\mathrm{PF_6}^-$ behave ideally in solution, $[\alpha]$ for the former should be 10% greater, as the observed rotations α (which should be equal for solutions of equal *molar* concentrations) are divided by grams per milliliter.

(50) Complex $\mathbf{2e}^+\mathrm{BF_4}^-$ was prepared from the chlorobenzene complex $[(\eta^5\text{-}\mathrm{C_5H_5})\mathrm{Re(NO)(PPh_3)(ClC_6H_5)}]^+\mathrm{BF_4}^-$ and isobutylene in a procedure analogous to those recently reported for gaseous alkynes.[13] The full characterization of salts $\mathbf{2e}^+\mathrm{SO_3F}^-$ and $\mathbf{2e}^+\mathrm{TfO}^-$ has been previously reported.[16,28] Complex $\mathbf{2e}^+\mathrm{BF_4}^-$ was obtained as a cream powder: 88%; mp 124–126 °C dec. Anal. Calcd for $\mathrm{C_{27}H_{28}BF_4NOPRe}$: C, 47.24; H, 4.11. Found: C, 47.42; H, 4.11.